21.6 A Multiband LTE SAW-less Modulator with -160dBc/Hz RX-Band Noise in 40nm LP CMOS

Vito Giannini[1], Mark Ingels[1], Tomohiro Sano[2], Bjorn Debaillie[1], Jonathan Borremans[1], Jan Craninckx[1]

[1]imec, Leuven, Belgium, [2]Renesas Electronics, Itami, Japan

In FDD cellular standards, the transmitter's out of-band noise leaks into the receive band due to the finite duplexer TX to RX isolation. If this noise is not low enough, a SAW filter is needed before the Power Amplifier to preserve the RX sensitivity. Out-of-band noise is also an important concern for coexistence of cellular transmitters with standards like GPS, WLAN and/or WiMAX on the same smart phone, a very common scenario nowadays. The *SAW-less* RX-band noise challenge becomes even more acute in the Long-Term Evolution (LTE) standard [1] where transmitters will need to operate in multiple FDD bands, using wider channel bandwidths and higher Peak-to-Average Power Ratios (PAPR).

CMOS transmitters with RX-band Carrier-to-Noise-Ratio (CNR) down to -160dBc/Hz were presented for the most popular WCDMA bands (I, II, V) in [2-6]: high-voltage Gilbert mixers [2] are generally power hungry whereas feedback-based notching techniques [3] are hard to implement for wider bandwidths and low TX-RX offsets. A direct quadrature voltage modulator was proposed in [4]: this upconversion technique uses the combination of an RC pole and passive mixer to achieve good noise performance with low power consumption. However, losses of such mixers are proportional to the passive pole's resistor value and, especially at high carrier frequencies, shift the linearity requirements to the baseband driving stage which should provide large linear signal swings on a low impedance node.

In this paper, the potential of voltage sampling is conceptually re-examined in a complete TX chain to cover all LTE-FDD bands and beyond, resulting in a highly efficient and flexible architecture. The presented transmitter achieves CNR down to -162dBc/Hz for channel bandwidths up to 20MHz in most LTE-FDD bands, including band XI (1.4GHz carrier/ 48MHz TX-RX offset frequency), band XII (0.7GHz / 30MHz) and band VII (2.5GHz / 120MHz), without the aid of external inter-stage acoustic filters. Furthermore, the same transmitter provides legacy with all WCDMA FDD scenarios and can be used with other bands/modulations such as GMSK and OFDM-based standards up to 5.5GHz carrier frequency.

Figure 21.6.1 shows the block diagram of the presented transmitter: a flexible 3rd-order transimpedance low-pass filter (TILPF) removes the DAC aliases and out-of-band quantization noise. The TILPF is followed by a passive mixer which upconverts the baseband voltage on the pre-power-amplifier's (PPA) input capacitor. To ease the interfacing with different Power Amplifiers, 2 on-chip baluns centered around 1GHz and 2GHz are integrated, together with a wideband differential output.

Figure 21.6.2 shows the schematic of both baseband and upconversion blocks. The TILPF design is based on a flexible Tow-Thomas topology that offers independent programming of transimpedance gain, bandwidth and quality factor, whereas a quadrature voltage sampling mixer passively performs the upconversion using a low-noise 25%-duty-cycle LO driver. Filtering and mixing stages are designed to limit the impact on the transmitter CNR while keeping the power consumption minimal over the required RF range. At baseband, to achieve out-of-band noise lower than -180dBVrms/Hz with limited power consumption, a passive LPF is added after the TILPF. From a system perspective, good CNR and high output power over different bands can be achieved with a tuneable passive pole (RPx-CP in Fig. 21.6.2). Special care must be put in selecting the right RP value which finally determines the losses of the passive mixer [6] and therefore the transmitter maximal frequency range. Low cut-offs and big RP values are needed for the lower RF frequencies with small TX-RX separation; on the other hand, RP should be as small as possible at high RF frequency and/or wide channel bandwidths. As shown in Fig. 21.6.2, to avoid linearity degradation, the switches of the RP array are closed inside a multi-feedback loop generated from the previous filtering stage. When an SP switch is ON to activate a certain resistor RPx, a corresponding feedback loop is selected through the switch SF and feedback resistor RF. The nonlinear resistance of the active SP switch is thus divided by the open loop gain of the TILPF making its contribution to the distortion negligible. Overall the passive pole bandwidth can vary from about 7MHz up

to 50MHz without sacrificing linearity. In order to efficiently drive RP values as low as 40Ω, a Class-AB low-voltage op-amp topology is implemented that can trade power consumption for linearity where needed.

Figure 21.6.3 shows the schematic of the PPA: it consists of a cascoded differential Common-Source amplifier loaded with 2 on-chip baluns with programmable center frequency. A wideband differential output is provided as well. The amplifier transistor is split in binary scaled units that can be turned on or off by thick-oxide cascode transistors. At the lower gain end, additional gain steps are obtained by dumping the part of the signal current into the power supply rather than in the selected output. Overall, the PPA gain range is 60dB, achieved in 11 coarse steps of 6dB. Fine gain control can be provided in the digital domain by adding 1 extra bit (6dB) in the DAC.

The transmitter is fabricated in a 40nm LP CMOS process. The core area is $1.4 \times 0.7mm^2$ (Fig. 21.6.7), mainly dominated by the baseband capacitors and the on-chip baluns. Figure 21.6.4.a shows measurements results of the transmitter gain versus the RF frequency: as discussed previously, the right selection of the resistor RP is critical to achieve sufficient gain and CNR in all LTE FDD bands. The big dots represent the best possible configuration achieving flat gain up to 3.5GHz. Figure 21.6.4.b shows the measured EVM as a function of the output power. It is better than 2.2% in WCDMA bands VII, XI and XII. LO feedthrough better than -40dBc is shown in Fig. 21.6.4.c. The transmitter consumes 13 to 44mA from the 1.1V supply (TILPF + LO generation) depending on the selected bandwidth and LO frequency, whereas the PPA consumes less than 43mA from the 2.5V (PPA), proportionally to the required output power and linearity. Figure 21.6.4.d shows the current consumption versus the output power in LTE band XII mode. Thanks to the scalable PPA current, the DG09 weighted power consumption for most WCDMA scenarios can be lower than 30mW.

Figure 21.6.5 shows EVM/ACLR measurements for a 20MHz bandwidth SC-FDMA LTE uplink operating in band II. An extensive overview of the measured performance in various operating modes, including the toughest WCDMA/LTE bands as well as GSM, WLAN and WiMAX, is given in Fig. 21.6.6. Output P_{1dB} is better than 10dBm in all modes except GSM, where we show how lower PPA linearity can be traded for current consumption. An EVM better than 2.5% is measured in WCDMA, LTE GSM and WiMAX modes. Finally, a CNR better than -160dBc/Hz is obtained, which is sufficient for SAW-less operation in all WCDMA/LTE FDD bands.

References:
[1] 3GPP TS 36.101, "Evolved Universal Terrestrial Radio Access (LTE): User Equipment (UE) Radio Transmission and Reception," v. 8.6.0, June 2009.
[2] M. Cassia et al., "A Low-Power CMOS SAW-Less Quad Band WCDMA/HSPA/HSPA+/ 1X/EGPRS Transmitter"', *IEEE Journal of Solid-State Circuits*, vol. 44, no. 7, pp. 1897-1906, July 2009.
[3] A. Mirzaei, H. Darabi; "A Low-Power WCDMA Transmitter With an Integrated Notch Filter", *IEEE Journal of Solid-State Circuits*, vol.43, no.12, pp.2868-2881, Dec. 2008.
[4] Xin He, J. van Sinderen, R. Rutten, "A 45nm WCDMA transmitter using direct quadrature voltage modulator with high oversampling digital front-end", *ISSCC Dig. Tech. Papers*, vol., no., pp.62-63, 7-11 Feb. 2010.
[5] K. Hausmann et al.; , "A SAW-less CMOS TX for EGPRS and WCDMA", *IEEE Radio Frequency Integrated Circuits Symposium (RFIC),* pp.25-28, May 2010.
[6] M. Ingels, V. Giannini, J. Borremans, et al. , "A 5mm² 40nm LP CMOS 0.1-to-3GHz Multistandard Transceiver", *ISSCC Dig. Tech. Papers*, pp.458-459, Feb. 2010.
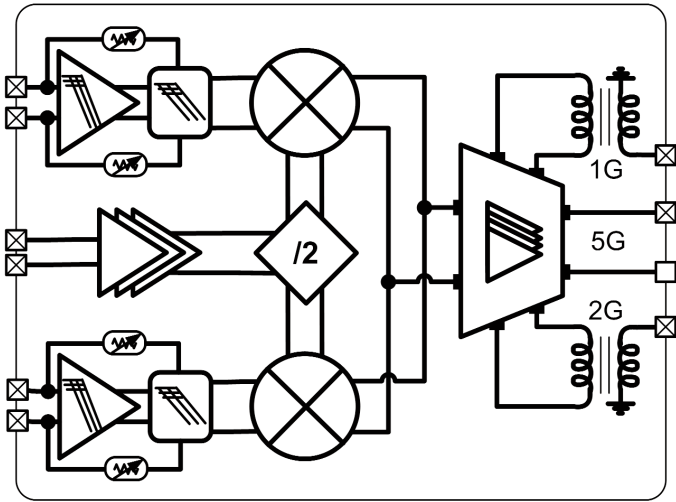
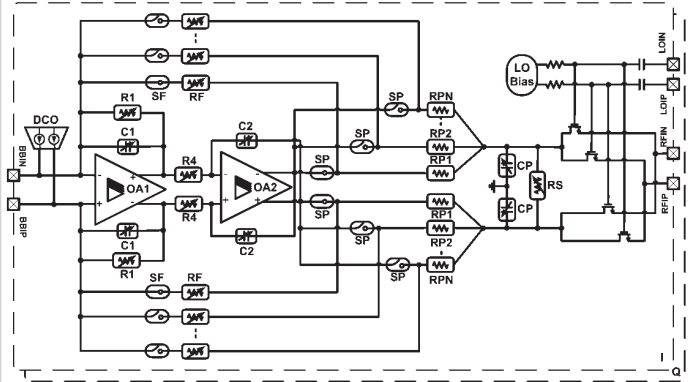**Figure 21.6.1: The multiband LTE Modulator block diagram.**

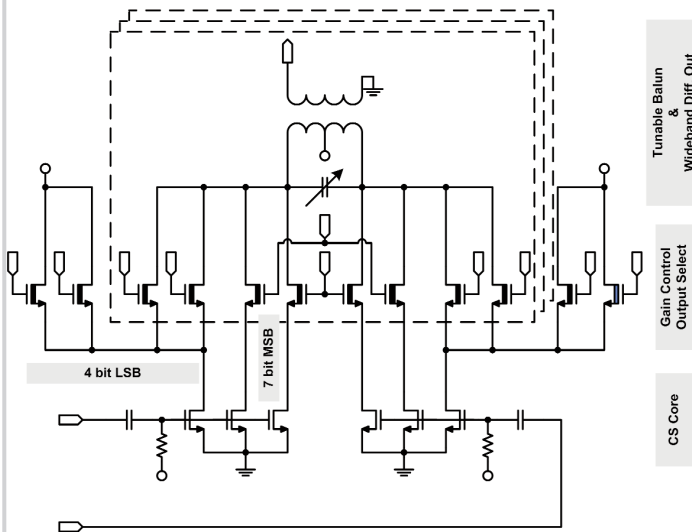**Figure 21.6.2: Flexible TIA and voltage-sampling mixer.**

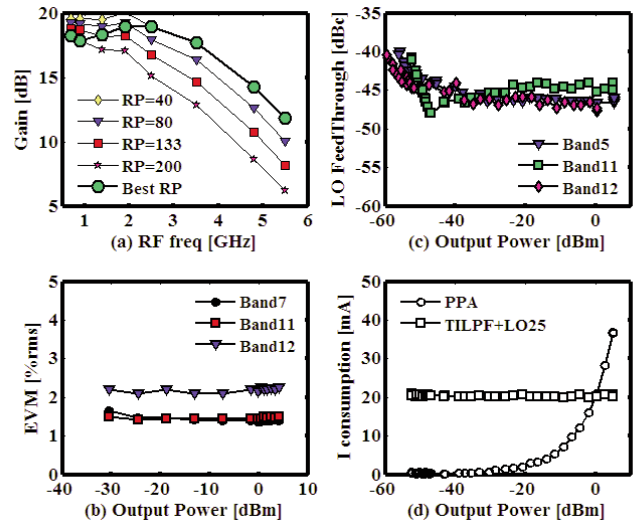**Figure 21.6.3: Multiband variable-gain Pre-Power Amplifier.**

Figure 21.6.4: Gain for different RP (a); EVM vs Pout in WCDMA (b); LOFT vs Pout in LTE (c); I consumption vs Pout for LTE Band11 (d).
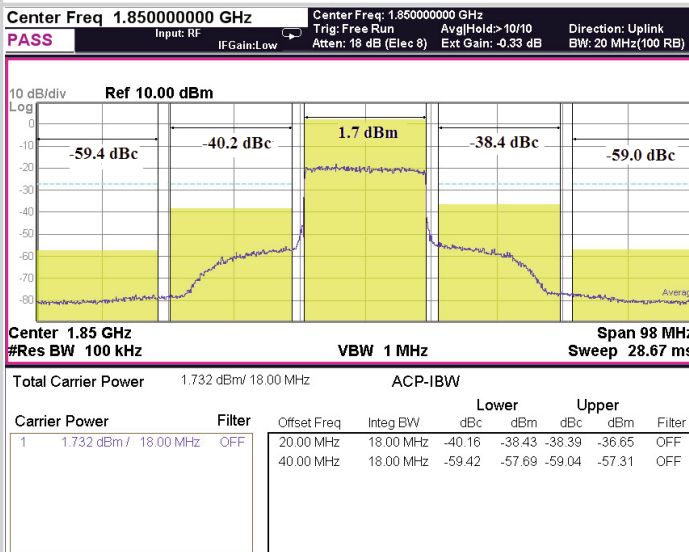

Figure 21.6.5: Spectral mask for LTE band II.

| Band # Fcarrier Δ TX-RX	Mode	BW [MHz]	OP1dB [dBm]	Pout [dBm]	EVM [%]	ACLR1/2 [dBc]	CNR [dBc/Hz]	Imax [mA] 1.1V/2.5V	DG.09 [mW]
Band I 1.92GHz 190MHz	UMTS	4	10.4	3.79	2.0	-40.2/-67	-162	21/41	30.9
	LTE	20	10.4	2.1	2.5	-39/-58	-160	25/40	
Band II 1.85GHz 80MHz	UMTS	4	10.4	4.39	2.3	-40.2/-63	-164	20/40	30.2
	LTE	20	10.4	2.6	2.4	-38.4/-59	-162.5	24/40	
Band V 0.82GHz 45MHz	UMTS	4	10.9	4.45	1.7	-41/-68	-161.7	14/37	24.8
	LTE	10	10.9	2.45	1.7	-41.4/-63	-160.5	17/37	
Band VII 2.5GHz 120MHz	UMTS	4	13.5	7.1	1.5	-46/-72	-159	24/40	38.5
	LTE	20	13.5	5.1	2	-42/-58	-158	28/40	
Band XI 1.42GHz 48MHz	UMTS	4	11.7	5.2	1.5	-41/-67	-162.6	18/37	27.8
	LTE	20	11.7	3.4	2.0	-42/-58	-160.4	21/36	
Band XII 0.7GHz 30MHz	UMTS	4	10.5	2.41	2.1	-39.5/-65	-160	13/34	24.8
	LTE	10	10.5	0.4	1.9	-41/-67	-159	17/33	
0.9GHz 20MHz	GSM	0.2	8.1	4.5	1.7	-54/-67	-160	18/25	
2.4GHz 100MHz	WLAN	40	13.6	4.6	3.3	-41/-54	-159	27/40	
3.5GHz 100MHz	WiMAX	20	12.6	3	1.8	-41/-54	-155	38/43	
4.8GHz 100MHz	WLAN	20	10.47	1	8.1	-42/-48	-156	44/39	

Figure 21.6.6: Performance summary.

21
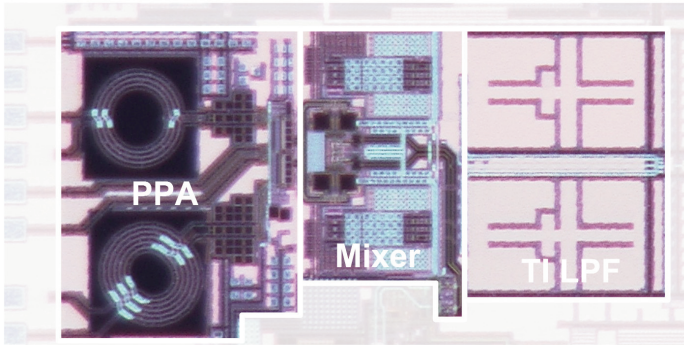
Figure 21.6.7: Chip micrograph of the transmitter.